Scientific Journal of Impact Factor (SJIF): 7.37

E-ISSN (O): 2348-4470
P-ISSN (P): 2348-6406

International Journal of Advance Engineering and Research Development

Volume 13,Issue 11,November 2026

Comparison of Adsorption Kinetics of Heavy Metals onto Plantain Stalk Activated Carbon

V.N. Nabie[1], C. Ukpaka[2] and N.D. Konee[1]

[1]Department of Chemical Engineering, Federal University of Environment and Technology, Koroma/Saakpenwa, Rivers State, Nigeria
[2]Department of Civil Engineering, Federal University of Environment and Technology, Koroma/Saakpenwa, Rivers State, Nigeria
Email: nabie.virginia@fuet.edu.ng, chinedu.ukpaka@fuet.edu.ng, konee.nulee.@fuet.edu.ng

ABSTRACT: *The adsorption mechanism and capacity of plantain stalk activated carbon (PSAC) in removing lead (II) ion (Pb^{2+}) and cadmium ion (Cd^{2+}) from aqueous solution was evaluated at different contact times. With 10 mg/L initial concentrations of Pb^{2+} and Cd^{2+}, pH 6, and 2g PSAC dosage, the percentage of Pb^{2+} and Cd^{2+} removed rapidly increased to 67.34% and 59.87% within 30 min and further to 99.17% and 98.04% after 180 min, indicating that Pb^{2+} was more adsorbed by PSAC than Cd^{2+}. The concentrations of the adsorbates removed after 120 min contact time was insignificant, implying that equilibrium was attained within 120 min. The experimental data were fitted to pseudo-first-order, pseudo-second-order, Elovich, and intra-particle diffusion models to determine the kinetics that best describe the mechanism of Pb^{2+} and Cd^{2+} adsorption onto PSAC. The evaluated k_1 and Q_e with pseudo-first-order model are 0.0518 min^{-1} and 2.4858 mg/g for Pb^{2+}, and 0.0506 min^{-1} and 4.2038 mg/g for Cd^{2+}, respectively, whereas the evaluated k_2 and Q_e values for pseudo-second-order model are 0.0486 g/mg.min and 1.3643 mg/g for Pb^{2+}, and 0.0312 g/mg.min and 1.4045 mg/g for Cd^{2+}. These indicate that the adsorption of Pb^{2+} onto PSAC is faster than that of Cd^{2+}. On the other hand, the equilibrium adsorption capacity (Q_e) for Pb^{2+} is less than that of Cd^{2+}, signifying that PSAC achieved a higher loading for Cd^{2+} than Pb^{2+} at equilibrium. The R^2 value (0.9973) for pseudo-second-order kinetic model is higher than those from the other models, indicating that the rate control mechanism for the adsorption is chemisorption. This was further validated by the better prediction accuracy of the adsorption capacity (Q_t) by the pseudo-second-order model compare to Elovich, intra-particle diffusion and pseudo-first-order models. Hence, the mechanism of Pb^{2+} and Cd^{2+} adsorption onto PSAC is dominantly chemisorption.*

KEYWORDS: *Adsorption, Activated Carbon, Heavy Metals, Kinetics, Comparison*

I. INTRODUCTION

Access to portable water for drinking is no easy despite water occupying around 70 % of the earth. The poor quality of water can be attributed to many human activities arising from urbanization, industrialization and poor waste management (Chie-Amadi *et al*., 2020; Ukpaka & Agunwamba, 2023 & Musti *et al*., 2025). Most anthropogenic activities release significant concentration of heavy metals in groundwater and surface water and due to the harmfulness of some heavy metals, drinking water needs to be properly treated before consumption (Dagde & Ndaka, 2019). Treatment of heavy metals requires effective technologies to reduce the concentration level below permissible limits. Adsorption method has proven to be one of the suitable methods for water treatment (Gaur *et al*., 2018; Yousif & Al-Mosawi, 2022).However, information about the reaction pathways and mechanisms of a sorption process can be determined through kinetic study. Several kinetic models are used to study the mechanism of an adsorption, such as the pseudo-first-order model, pseudo-second-order model, Elovich model, and intra-particle diffusion model. The fitting of these models to experimental data determines whether the rate controlling step for adsorption of contaminants onto an adsorbent is chemisorption, physisorption, or intra-particle diffusion (Raji *et al*., 2023). The pseudo-first-order and second-order kinetic model are used to explain the rate-limiting step for an adsorption study, while the Elovich model explains the heterogeneity of an adsorbent, describing the chemisorption of non-uniform site of the surface. On the other hand, intra-particle diffusion model explains the diffusion mechanism of adsorbate into the pores of an adsorbent (Tahir *et al*., 2026). The equilibrium adsorption capacity can also be evaluated from the pseudo-first-order and pseudo-second-order kinetic models (Azizi, *et al*., 2017; Nabie et al., 2026; Dagde & Ndaka, 2019).

@IJAERD-2026, All rights Reserved

The mechanism of an adsorption process can be influenced by the nature and type of adsorbents. However, many researchers have shown that the mechanism of adsorption of heavy metals, such lead (II) ion and cadmium (II) ion mostly dominated by chemisorption (Chie-Amadi *et al*., 2020; Tahir *et al*., 2026). Therefore, this present study evaluated the mechanism of Pb^{2+} and Cd^{2+} adsorption onto plantain stalk activated carbon (PSAC) by fitting experimental data to pseudo-first-order, pseudo-second-order, Elovich, and intra-particle diffusion models. The kinetic models were also used to predict the adsorption capacity of Pb^{2+} and Cd^{2+} onto PSAC at different contact times to determine the kinetic model that has the most prediction accuracy.
The study is aimed at investigating the adsorption mechanism and capacity of plantain stalk activated carbon (PSAC) in removing lead (II) ion (Pb^{2+}) and cadmium ion (Cd^{2+}) from aqueous solution different contact times.

II. MATERIALS AND METHODS

2.1 Materials

The materials are plantain stalk, graduated beaker, sieve, funnels, distilled water, test tubes, desiccators, digital weighing balance, grinder, filter papers, conical flasks, rotary disc, spatula, oven, measuring cylinder, crucibles, thermometer, pH meter, stop watch, Atomic Absorption Spectrophotometer (AAS), sodium hydroxide (NaOH), phosphoric acid (H_3PO_4), sodium thiosulphate ($Na_2S_2O_3.5H_2O$), hydrochloric acid (HCl), lead(II) nitrate ($Pb(NO_3)_2$) and cadmium chloride ($CdCl_2$).

2.2 Sample Collection and Preparation

Plantain stalks (false horn variety stalks) were collected from the Oil-mill market in Rumukwurushi, Obio/Akpor Local Government Area of Rivers State, Nigeria. The samples were cut into small pieces, washed thoroughly with water to remove dirt particles, and oven-dried at 105 ºC for 24 hours.

2.3 Carbonization and Activation

The dried plantain samples were prepared and activated according to the methods described by Dechapanya and Khamwichit (2023) with slight modifications. The dried samples were carbonized in a muffle furnace at 420 ºC for 75 minutes, and then pulverized to a fine powder. 100 g of the pulverized samples was mixed with 85% v/v H_3PO_4 in a beaker and stirred until a consistent paste was obtained. This was transferred into a bowl and kept for 24 hours. The settled sample was drained and activated by cooking at 100 ºC for 3 hours. After the activation, the sample was cooled and washed with distilled water until the pH was neutral. The final sample was oven-dried at 105 ºC for 24 hours to a constant weight and then stored in airtight containers.

2.4 Preparation of Heavy Metal Concentration

Batch experiments were conducted at various initial concentrations of lead (Pb^{2+}) and cadmium (Cd^{2+}) ions to study the effects of initial concentration on the adsorption kinetics of Pb^{2+} and Cd^{2+} on the plantain stalk activated carbon (PSAC). A stock solution of Pb^{2+} ion and Cd^{2+} ion was prepared by weighing 1.60g of lead (II) trioxonitrate (V) ($Pb(NO_3)_2$) and 1.63g of cadmium chloride ($CdCl_2$) into 1000 ml volumetric flasks. Distilled water was added up to the required mark. 10 mg/L initial concentrations of Pb^{2+} and Cd^{2+} ions were prepared by diluting the stock further with distilled water.

2.5 Adsorption Experiment

250 mL distilled water was added to a conical flask, followed by the addition of the prepared aqueous solution of Pb^{2+} and Cd^{2+} ions. The content was vigorously stirred. Thereafter, a 2 g of the plantain stalk activated carbon (PSAC) was added and stirred. The pH of the solution was adjusted to 6.0 using NaOH and HCl. The flask was placed on a magnetic rotary disc connected to a power source. The power was switched on to vigorously agitate the solution at 100 rpm. This experiment was conducted at room temperature (approximately 30 ºC). The overall contact for the experiment was 180 minutes. Every 30 minutes, a 10 mL sample was drawn from the solution via a syringe. The collected sample was filtered through filter paper and analysed using an atomic absorption spectrophotometer (AAS) to determine the concentrations of Pb^{2+} and Cd^{2+} ions adsorbed by the adsorbent.

2.6 Kinetics of the Adsorption Process

The adsorption kinetics adopted in this study include Lagergren's pseudo-first-order and second-order equations, Elovich and intra-particle diffusion models. The experimental data were fitted into the kinetic models to ascertain the model with the best fit to the adsorption of Pb^{2+} and Cd^{2+} ions onto PSAC adsorbent.

@IJAERD-2026, All rights Reserved

2.6.1 Pseudo First Order Kinetics

Lagergren's pseudo-first-order equation is expressed by Ho (2004) as:

$$\frac{dQ_t}{dt} = k_1(Q_e - Q_t) \quad (1)$$

where:

k_1 =Pseudo first-order adsorption rate constant (min^{-1})
Q_e = Concentration of heavy metal adsorbed by the adsorbent at equilibrium (mg/g)
Q_t = Concentration of heavy metal adsorbed by the adsorbent with time (mg/g)
t = Measured time of adsorption (min)

Integrating equation (1) yields the final expression as:

$$ln(Q_e - Q_t) = ln\, Q_e - k_1 t \quad (2)$$

Plotting $ln(Q_e - Q_t)$ against t gives a straight-line equation with slope as k_1 and intercept as $ln\, Q_e$. From the regression equation displayed on the plotted graph, the values of k_1 and Q_e were obtained. The concentration of heavy metal adsorbed by the adsorbent at any time (Q_t) can be predicted by transforming equation (2) to give:

$$Q_t = Q_e(1 - e^{-k_1 t}) \quad (3)$$

2.6.2 Pseudo Second Order Kinetics

Similarly, the pseudo-second order kinetic model is expressed by Ho and McKay (1999) as:

$$\frac{dQ_t}{dt} = k_2(Q_e - Q_t)^2 \quad (4)$$

where:

k_2 =Pseudo-second order adsorption rate constant (g/mg.min)

Again, integrating equation (4) yields the final equation as:

$$\frac{t}{Q_t} = \frac{t}{Q_e} + \frac{1}{Q_e^2 k_2} \quad (5)$$

Plotting $\frac{t}{Q_t}$ against t give a straight-line equation with slope as $\frac{1}{Q_e}$ and intercept as $\frac{1}{Q_e^2 k_2}$. From the regression equation displayed on the plotted graph, the values of k_2 and Q_e were determined.

The concentration of heavy metal adsorbed by the adsorbents at any time (Q_t) can be predicted by rearranging equation (5) to give:

$$Q_t = \frac{k_2 Q_e^2 t}{1 + k_2 Q_e t} \quad (6)$$

2.6.3 Elovich Kinetic Model

The Elovich model is another model used to evaluate mechanism of an adsorption process. A fitted experimental implies that adsorption is chemisorption (Manjuladevi *et al*., 2018; Zand & Abyaneh, 2020; Raji *et al*., 2023). It is expressed as:

$$Q_t = \frac{1}{\beta} ln(\beta \alpha t) \quad (7)$$

where:

Q_t = The adsorption capacity at time t (mg/g)
β =Constant denoting the extent of surface coverage (g/mg)

@IJAERD-2026, All rights Reserved

α = Initial adsorption rate (mg/g.min)
t =Contact time (min)

Further simplification of equation (7) gives the linear form (Khamwichit *et al*., 2022) as:

$$Q_t = \frac{1}{\beta} ln(\beta\alpha) + \frac{1}{\beta} ln\, t \quad (8)$$

Plotting Q_t against $ln\, t$, the constants are determined from the graph. Thus, the slope of the graph is equivalent to $\frac{1}{\beta}$, from which the extent of surface coverage (β) is evaluated, while the initial adsorption rate (α) is determined from the intercept, $\frac{1}{\beta} ln(\beta\alpha)$.

2.6.4 Intra-Particle Diffusion Model

The intra-particle diffusion model (Adeogun *et al*., 2013) is expressed as:

$$Q_t = K_d\sqrt{t} + \varepsilon \quad (10)$$

where: Q_t = The amount adsorbed at time t (mg/g)
K_d = Weber and Morris intra-particle diffusion rate constant (mg/g.min$^{0.5}$)
ε = Constant related to adsorption capacity (mg/g)
t =Time of adsorption (min)

Plotting Q_t against$\sqrt{t}$ gives a straight-line equation. The slope or coefficient of the regression equation is equated to K_d, while its value is determined for each experiment. It is worthy of note that when the straight line does not pass through the origin of the graph, the adsorption process can be described as intra-particle diffusion, but if it does not, then intra-particle diffusion is not the rate-controlling step (Ademiluyi & Ujile, 2013).

The adsorption capacity at equilibrium was calculated using the formula:

$$Q_e = (C_i - C_e)\frac{V}{w} \quad (11)$$

The adsorption capacity at any time was calculated using the formula:

$$Q_t = (C_i - C_t)\frac{V}{w} \quad (12)$$

where:
Q_e = Adsorption capacity at equilibrium (mg/g)
Q_t = Adsorption capacity at time, *t* (mg/g)
C_i = Initial concentration of metal ion in the solution (mg/L)
C_e = Concentration of metal ion in the solution at equilibrium (mg/L)
C_t = Concentration of metal ion in the solution at time, *t* (mg/L)
V =Volume of solution (L)
w =Weight of adsorbent (g)

III. RESULTS AND DISCUSSION

3.1 Adsorption Efficiency of PSAC

The capacity of PSAC in adsorbing Pb^{2+} and Cd^{2+} ions has been demonstrated experimentally, as shown in Table 1.

Table 1: Removal of Pb^{2+} and Cd^{2+} by the adsorbent

Time (min)	Pb (%)	Cd (%)
30	67.34	59.87
60	87.6	82.09

@IJAERD-2026, All rights Reserved

90	96.97	91.81
120	98.86	96.59
150	99.08	97.81
180	99.17	98.04

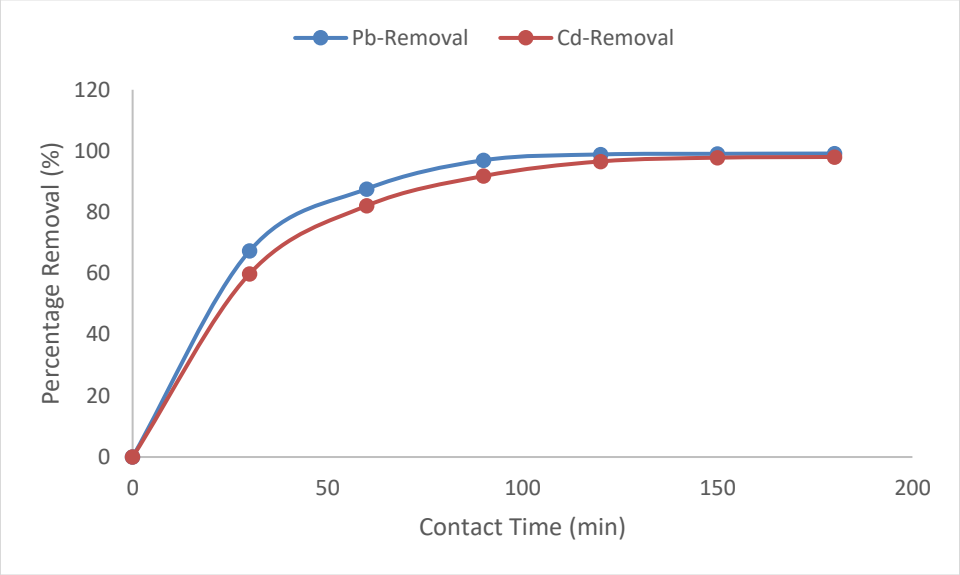


Figure 1: Removal of Pb^{2+} and Cd^{2+} by PSAC at various contact times

Figure 1 shows the profile of Pb^{2+} and Cd^{2+} removal percentages at different contact times. The percentage removal of both metals increased with contact time until equilibrium was reached. From Table 1, the percentage of Pb^{2+} and Cd^{2+} removed by PSAC increased markedly from 67.34% and 59.87% within 30 min to 99.17% and 98.04% after 180 min. Equilibrium is attained within 120 min for both metals, but the amount of Pb^{2+} removed by the adsorbent is slightly higher than that of Cd^{2+}. The rapid and continuous uptake of contaminants is common in the adsorption process. This rapid increase in removal efficiency of the metals within a few minutes of adsorption indicates that the adsorption progresses through three distinct phases, which are the initial and fast external mass transfer phase, the gradual intra-particle diffusion-controlled phase, and the equilibrium phase where adsorption sites have become saturated (Almanassra et al., 2022).

The removal efficiency of both metals is consistent with adsorption studies. Akinyeye et al. (2020) observed initial rapid adsorption of Pb^{2+} and Cd^{2+} onto bamboo stem biomass, with equilibrium established after 60 min. Almanassra et al. (2022) also reported a similar trend for Pb^{2+} adsorption using rice husk adsorbent, with equilibrium attained within 400 min, while Tahir et al. (2026) showed that Pb^{2+} and Cd^{2+} adsorption onto buckwheat hulls adsorbent increased rapidly within the first few minutes and then stabilized, reaching equilibrium within 180 min. Overall, PSAC effectively adsorbed Pb^{2+} and Cd^{2+} ions from contaminated water.

3.2 Kinetic Rate Parameters

The experimental data were fitted to pseudo-first-order, pseudo-second-order, Elovich, and intra-particle diffusion models to determine the kinetics that best describe the mechanism of Pb^{2+} and Cd^{2+} adsorption onto PSAC. The displayed regression equations in Figures 2 to 5 were compared with equations (2), (5), (8) and (10) to determine the constants of the respective equations.

@IJAERD-2026, All rights Reserved

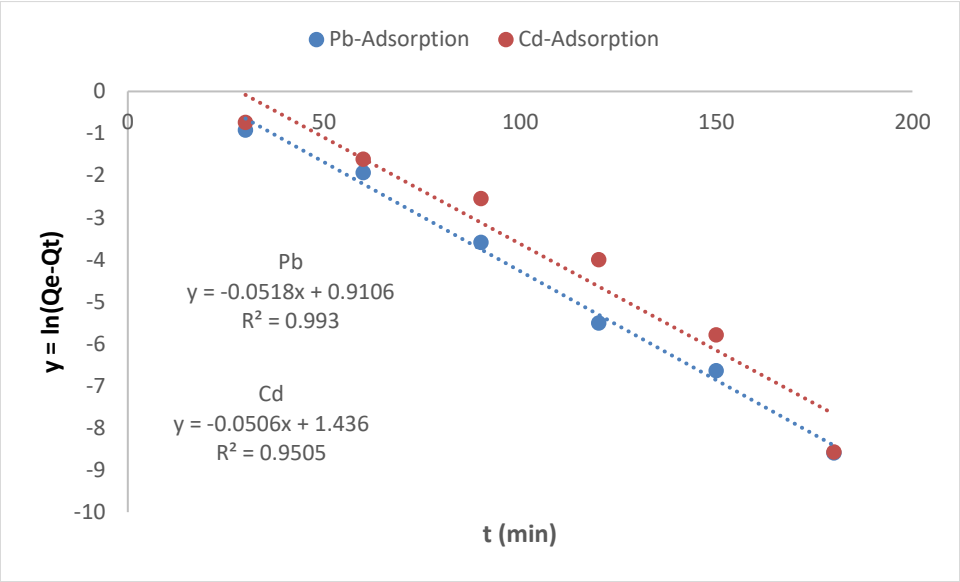


Figure 2: Plot of pseudo-first-order kinetic model for determination of constants

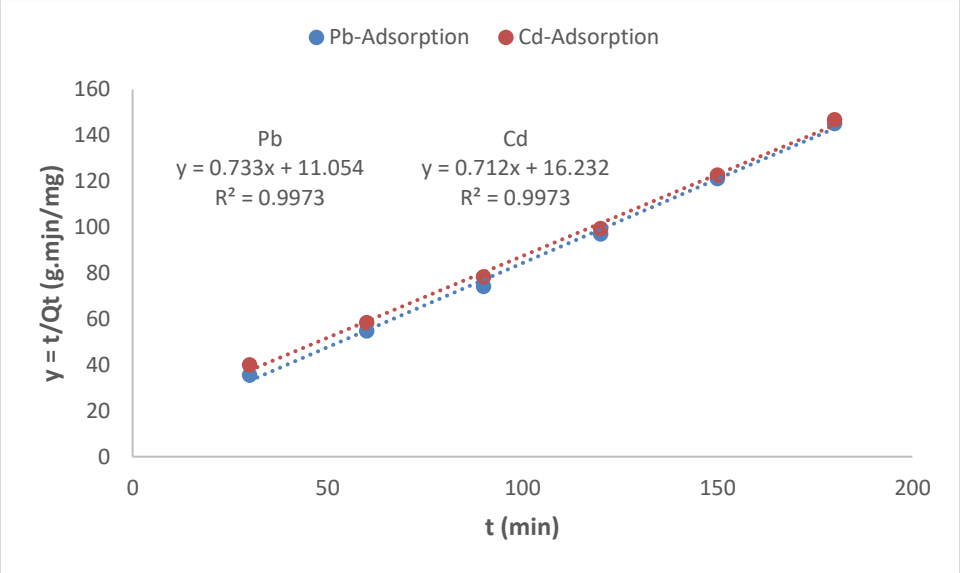


Figure 3: Plot of pseudo-second-order kinetic model for determination of constants

@IJAERD-2026, All rights Reserved

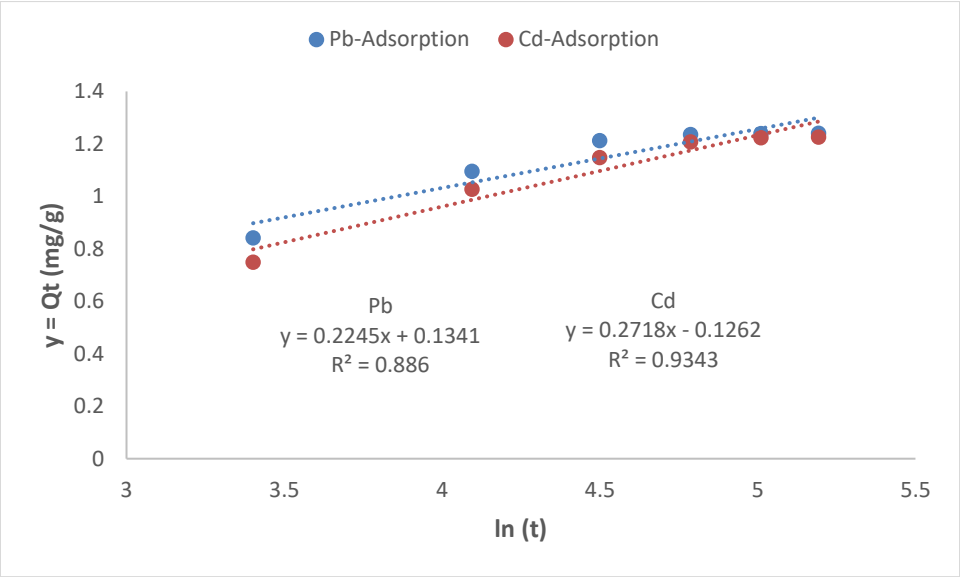


Figure 4: Plot of Elovich kinetic model for determination of constants

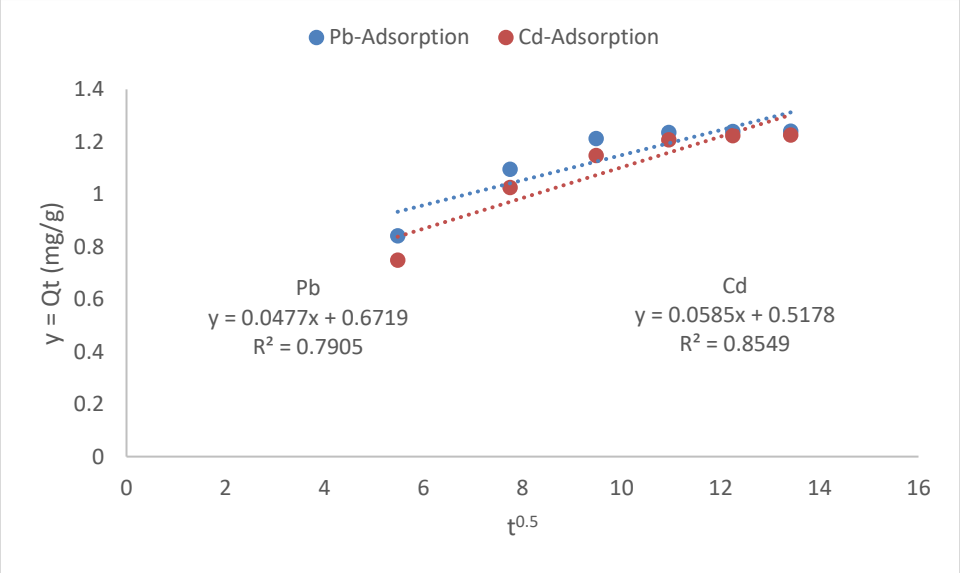


Figure 5: Plot of intra-particle diffusion model for determination of constants

Figure 2 shows the plot of experimental data fitted to the pseudo-first-order kinetic model. The displayed regression equations were compared with equation (2) to determine the first-order kinetic rate constant (k_1) and equilibrium adsorption capacity (Q_e) for Pb^{2+} and Cd^{2+} ions adsorption. The evaluated k_1 and Q_e values are shown in Table 1. As shown in Table 1, the values of k_1 and Q_e for Pb^{2+} adsorption are 0.0518 min^{-1} and 2.4858 mg/g, respectively, whereas k_1 and Q_e values for Cd^{2+} adsorption were determined as 0.0506 min^{-1} and 4.2038 mg/g, respectively. In addition, the coefficient of determination (R^2) is 0.9930 for Pb^{2+} and 0.9505 for Cd^{2+}. Similarly, Figure 3 shows the plot of experimental data fitted to the pseudo-second-order kinetic model, with the displayed regression equations used for the determination of k_2 and Q_e. The evaluated k_2 and Q_e values are shown in Table 2, which are 0.0486 g/mg.min and 1.3643 mg/g for Pb^{2+}, and 0.0312 g/mg.min and 1.4045 mg/g for Cd^{2+}, with R^2 of 0.9973 for both Pb^{2+} and Cd^{2+}.

Furthermore, by comparing the regression equations in Figure 4 with equation (8), the initial adsorption rate (α) and extent of surface coverage (β) of the Elovic model were evaluated as shown in Table 1. Thus, the value of α was evaluated as 0.4080 mg/g.min for Pb^{2+} adsorption and 0.1708 mg/g.min for Cd^{2+} adsorption, while β was evaluated

@IJAERD-2026, All rights Reserved

as 4.4543 g/mg for Pb^{2+} adsorption and 3.6792 g/mg·min for adsorption of Cd^{2+}. Also, utilising the regression equations in Figure 5, after comparing with equation (10), the intra-particle diffusion rate constant (K_d) was evaluated as 0.0477 mg/g.$min^{0.5}$ for Pb^{2+} adsorption and 0.0585 mg/g.$min^{0.5}$ for Cd^{2+} adsorption.

The pseudo-first-order and second-order kinetic rate constants for Pb^{2+} and Cd^{2+} adsorption onto PSAC are within the range reported in similar studies using different biosorbents, such as maize husk (Adeogun *et al*., 2013), tiger nut (Adewale *et al*., 2024), and *Ximenia americana L*. (Cardoso *et al*., 2025). The values of the rate constants are higher for adsorption Pb^{2+} compared to Cd^{2+}, indicating that the adsorption of Pb^{2+} onto PSAC is faster than the uptake of Cd^{2+} in aqueous solution. On the other hand, the equilibrium adsorption capacity for Pb^{2+} is less than that of Cd^{2+} for both kinetic rates. This signifies that while PSAC adsorbed Pb^{2+} at faster rate, it reaches higher loading for Cd^{2+} than Pb^{2+} at equilibrium. Similar studies also reported higher Q_e values in adsorption of Cd^{2+} than Pb^{2+} (Akinyeye *et al*., 2020; Adewale *et al*., 2024).

Generally, the pseudo-second-order kinetic rate exhibited higher coefficient of determination (R^2) compared to the other models. This implies that the rate-limiting step for adsorption of Pb^{2+} and Cd^{2+} onto PSAC adsorbent is a chemisorption, which involves exchange of electrons between the adsorbent and the adsorbate (Tahir *et al*., 2026). Thus, this justifies the closeness of the estimated Q_e from second-order model to the Q_e calculated from the experiment (1.2398 mg/g for Pb^{2+} and 1.2257mg/g for Cd^{2+}) than the Q_e obtained from the pseudo-first-order model.

Furthermore, the R^2 values obtained from the Elovich and intra-particle diffusion models are lower compare to the pseudo-second-order kinetic model. Nevertheless, the relatively high coefficients signify that the adsorption of Pb^{2+} and Cd^{2+} is a non-uniform chemisorption process, while the intra-particle diffusion model implies that the metals also diffused into the PSAC pores, but not the sole rate-controlling step, as the plot in Figure 5 did not pass through the origin. Similar studies have shown that intra-particle diffusion is not the sole rate-controlling step for adsorption of Pb^{2+} or Cd^{2+}, but also occurred as a boundary layer diffusion (Al-Ma'abreh *et al*., 2024; Tahir *et al*., 2026). Table 2 summarises the kinetic rate parameters and the equilibrium adsorption capacity estimated from the models.

Table 2: Summary of kinetic rate parameters for Pb^{2+} and Cd^{2+} adsorption

	Pseudo-first-order			**Pseudo-second-order**		
Metal ion	**k_1 (min^{-1})**	**Q_e (mg/g)**	**R^2**	**k_2 (g/mg.min)**	**Q_e (mg/g)**	**R^2**
Pb	0.0518	2.4858	0.9930	0.0486	1.3643	0.9973
Cd	0.0506	4.2038	0.9505	0.0312	1.4045	0.9973
	Elovich			**Intra-Particle Diffusion**		
Metal ion	**α (g/mg.min)**	**β (g/mg)**	**R^2**	**K_d (mg/g.$min^{0.5}$)**	**ε (mg/g)**	**R^2**
Pb	0.4080	4.4543	0.8860	0.0477	0.6719	0.7905
Cd	0.1708	3.6792	0.9343	0.0585	0.5178	0.8549

3.3 Adsorption Capacity of PSAC Adsorbent

The performance of the kinetic models was tested by predicting the capacity of PSAC in adsorbing Pb^{2+} and Cd^{2+} from the aqueous solution at a given contact time. the predicted adsorption capacities are illustrated in Figures 6 and 7.

@IJAERD-2026, All rights Reserved

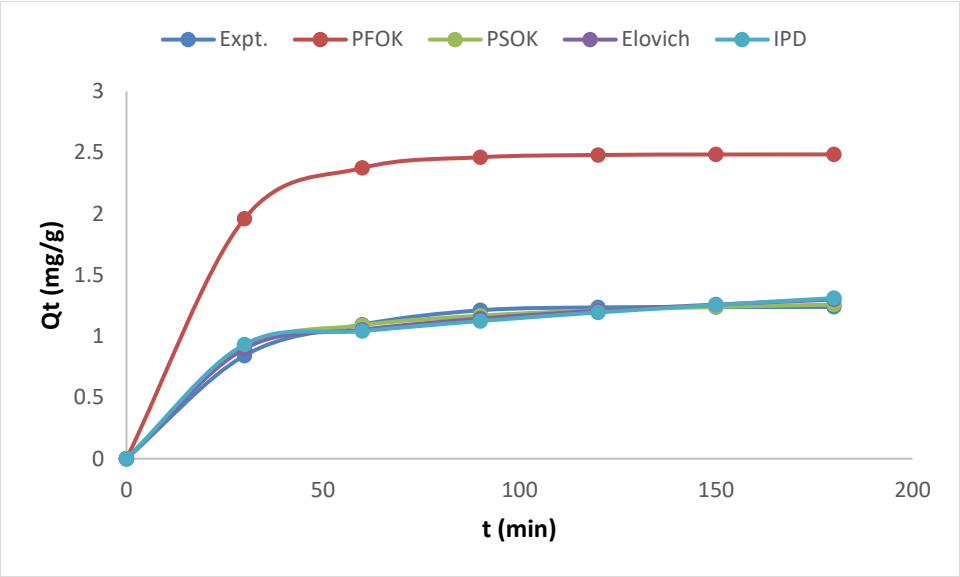


Figure 6: Predicted Q_t for Pb^{2+} adsorption onto PSAC adsorbent

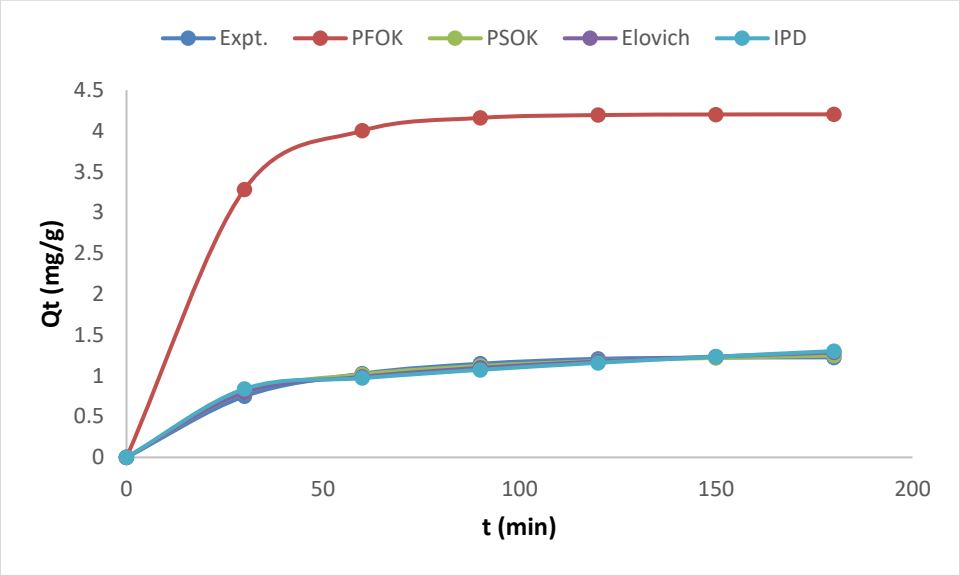


Figure 7: Predicted Q_t for Cd^{2+} adsorption onto PSAC adsorbent

Figures 5 and 6 show the comparison of predicted adsorption capacity (Q_t) of Pb^{2+} and Cd^{2+} ions by the pseudo-first-order kinetics (PFOK), pseudo-second-order kinetics (PSOK), Elovich and intra-particle diffusion (IPD) model. The predicted Q_t by the respective models and the calculated Q_t from the experiment (Expt.) are presented in Table 3. The Q_t values predicted for Pb^{2+} and Cd^{2+} by the pseudo-first-order kinetic model significantly deviated from the experimentally calculated Q_t as illustrated in Figures 5 and 6. Thus, the profiles representing FPOK drifted away from the experimental Q_t. This suggests that the adsorption of Pb^{2+} and Cd^{2+} onto PSAC is not physisorption, or surface-driven kinetics. Hence, the pseudo-first-order model cannot accurately describe the mechanism of Pb^{2+} and Cd^{2+} adsorption onto PSAC.

On the other hand, predicted Q_t values by the pseudo-second-order kinetic model, Elovich model, and intra-particle diffusion model were close to the calculated experimental Q_t values for any given contact time. This is demonstrated in the Figures 5 and 6. The estimated root mean squared error (RMSE) further substantiated deviation between the PFOK predicted Q_t and the experiment. The RMSE values between predicted Q_t and experimental Q_t for Pb^{2+}

@IJAERD-2026, All rights Reserved

adsorption are 1.2321 for PFOK, 0.0347 for PSOK, 0.0487 for Elovich and 0.0660 for IPD. Similarly, for Cd^{2+} adsorption, the RMSE values between predicted Q_t and experimental Q_t are 2.9159 for PFOK, 0.0273 for PSOK, 0.0436 for Elovich and 0.0648 for IPD. Generally, the error analysis showed that the pseudo-second-order kinetic (PSOK) model outperformed the other models, which is closely followed by the Elovich, and intra-particle diffusion model. The pseudo-first-order kinetic model shows the most deviated from the experiment. Hence, based on the degree of predictions and least error from the pseudo-second order kinetic model and Elovich model, it can be concluded that the rate control mechanism for adsorption of Pb^{2+} and Cd^{2+} onto PSAC is a chemisorption with strong interaction of functional groups at the PSAC surface.

Table 3: Comparison of predicted Qt (mg/g) for Pb^{2+} and Cd^{2+} adsorption

	Qt (mg/g) for Pb^{2+}					Qt (mg/g) for Cd^{2+}				
Time (min)	**Expt.**	**PFOK**	**PSOK**	**Elovich**	**IPD**	**Expt.**	**PFOK**	**PSOK**	**Elovich**	**IPD**
30	0.8418	1.9603	0.9079	0.8977	0.9332	0.7484	3.2826	0.7980	0.7982	0.8382
60	1.0950	2.3747	1.0903	1.0533	1.0414	1.0261	4.0020	1.0178	0.9866	0.9709
90	1.2121	2.4623	1.1685	1.1443	1.1244	1.1476	4.1596	1.1206	1.0968	1.0728
120	1.2358	2.4809	1.2120	1.2089	1.1944	1.2074	4.1942	1.1803	1.1750	1.1586
150	1.2385	2.4848	1.2396	1.2590	1.2561	1.2226	4.2017	1.2192	1.2357	1.2343
180	1.2396	2.4856	1.2588	1.2999	1.3119	1.2255	4.2034	1.2466	1.2852	1.3027

IV. CONCLUSION

The adsorption of Pb^{2+} and Cd^{2+} ions onto plantain stalk activated carbon (PSAC) is dependent on contact time. The percentage of Pb^{2+} and Cd^{2+} removed increased rapidly to 67.34% and 59.87% within 30 min and further to 99.17% and 98.04% after 180 min, indicating that Pb^{2+} was more adsorbed by PSAC than Cd^{2+}. The study observed that equilibrium was attained within 120 min for both metals

The values of k_1 and k_2 are higher for adsorption Pb^{2+} compared to Cd^{2+}, indicating that the uptake of Pb^{2+} onto PSAC is faster than the uptake of Cd^{2+}. Conversely, the value of Q_e for Pb^{2+} is less than that for Cd^{2+}, signifying that PSAC achieved a higher loading for Cd^{2+} than Pb^{2+} at equilibrium. However, the estimated Q_e from the pseudo-second-order model is close to the Q_e calculated from the experiment than the pseudo-second-order model.

The R^2 value (0.9973) from pseudo-second-order kinetic model is higher than the values obtained from the pseudo-first-order, Elovich, and intra-particle diffusion models, indicating that the rate control mechanism for adsorption of Pb^{2+} and Cd^{2+} onto PSAC is chemisorption with strong interaction of functional groups on the PSAC surface. This was further validated by the better prediction accuracy of the adsorption capacity (Q_t) by the pseudo-second-order kinetic model compare to Elovich, intra-particle diffusion and pseudo-first-order kinetic models. Hence, the mechanism of Pb^{2+} and Cd^{2+} adsorption onto PSAC is dominantly chemisorption, with diffusion of the adsorbates into the PSAC particles also occurring in the process.

REFERENCES

[1]. Ademiluyi, F. T., & Ujile, A. A. (2013). Kinetics of batch adsorption of iron II ions from aqueous solution using activated carbon from Nigerian bamboo. International Journal of Engineering and Technology, 3(6), 623-631. Adeogun, A.I., Idowu, M.A., Ofudje, A.E., Kareem, S.O., and Ahmed, S.A. “Comparative biosorption of Mn(II) and Pb(II) ions on raw and oxalic acid modified maize husk: kinetic, thermodynamic and isothermal studies.” Appllied Water Science 3 no. 1 (2013):167–179.

[2]. Adewale, O.R., Olubunmi, S.M., Owolabi, S.A., Lawrence, O.O., Omotunde, T.O., Seun, O.T., Omololu, E.A., Omoniyi, O.O, Olaiwola, M.A., Onwordi, C.T., and Ayemu, A.A. “Kinetics, thermodynamic and isotherms modeling of the equilibrium sorption of Pb (II), Ni (II), and Cd (II) ions into tiger nut chaff (*Cyperus esculentus*) from model wastewater.” *Physical Chemistry* 13 no. 2 (2024): 19-31.

[3]. Akinyeye, O.J., Ibigbami, T.B., Odeja, O.O., & Sosanolu, O.M. (2020). Evaluation of kinetics and equilibrium studies of biosorption potentials of bamboo stem biomass for removal of Lead (II) and Cadmium (II) ions from aqueous solution. *African Journal of Pure and Applied Chemistry*, 14(2), 24-41.

@IJAERD-2026, All rights Reserved

[4]. Al-Ma'abreh, A.M., AlKhabbas, M., Alawaideh, S., Hussein-Al-Ali, S.H., Hmedat, D.A., Edris, G., Abuassaf, R.A., & Hamed, M.A. (2024). Investigation of kinetics, thermodynamics, and isotherms of the simultaneous removal of heavy metal ions by activated carbon from cypress fruit. *Adsorption Science & Technology*, 42, 1–15.
[5]. Almanassra, I.W., Khan, M.I., Atieh, M.A., & Shanableh, A. (2022). Adsorption of lead ions from an aqueous solution onto NaOH-modified rice husk. *Desalination and Water Treatment*, 262, 152–167.
[6]. Azizi, S., Shahri, M. M., & Mohamad, R. (2017). Green synthesis of zinc oxide nanoparticles for enhanced adsorption of lead ions from aqueous solutions: Equilibrium, kinetic and thermodynamic studies. *Molecules*, 22(6), 831.
[7]. Cardoso, R.S., Souza, C.O., Silva, D.B., Lima, L.R., Menezes, J.M.C., Lima, M.R.P., Gomes, H.O., Santos, Y.T.C. Filho, F.J.P., Coutinho, H.D.M., & Teixeira, R.N.P. (2025). Removal of the metal ion lead II from aqueous effluents using the stem bark of *Ximenia americana* L. *ACS Omega*, 10,40872−40885.
[8]. Chie-Amadi, G. O., Amagbo, L. G., & Walter, C. (2020). Performance of plantain pseudo stem for Pb+2 adsorption in aqueous solution. *European Journal of Advances in Engineering and Technology*, 7(4), 36-44.
[9]. Dagde, K. K., & Ndaka, J. I. (2019). Kinetic study of garlic and ginger particles in adsorption of heavy metals in aqueous solution. *Chemical and Process Engineering Research*, 60, 25-38.
[10]. Dechapanya W, Khamwichit, A: Biosorption of aqueous Pb(II) by H_3PO_4-activated biochar prepared from palm kernel shells (PKS). *Heliyon*. 2023, 9(1), e17250.
[11]. Gaur, N., Kukreja, A., Yadav, M., & Tiwari, A. (2018). Adsorptive removal of lead and arsenic from aqueous solution using soya bean as a novel biosorbent: Equilibrium isotherm and thermal stability studies. *Applied Water Science*, 8(6), 98.
[12]. Ho, Y. S. (2004). Citation review of Lagergren kinetic rate equation on adsorption reactions. Scientometrics, 59(1), 171-177.
[13]. Khamwichit, A., Dechapanya, W., & Dechapanya, W. (2022). Adsorption kinetics and isotherms of binary metal ion aqueous solution using untreated venus shell. *Heliyon*, 8, e09610.
[14]. Nabie, V.N., Ukpaka, C.P. & Dagde, K.K. (2026). Thermodynamics of Pb^{2+} and Cd^{2+} Ions adsorption onto plantain trunk activated carbon. International Journal of Trend in Research and Development, Volume 13(5), ISSN: 2394-9333.
[15]. Manjuladevi, M., Anitha, R., & Manonmani, S. (2018). Kinetic study on adsorption of Cr(VI), Ni(II), Cd(II) and Pb(II) ions from aqueous solutions using activated carbon prepared from Cucumis melo peel. *Applied Water Science*, 8, 36.
[16]. Musti, Y.A., Yaumi, A.L., Mukhtar, F.U., Highina, B.K., & Umar, H. (2025). Adsorption isotherms and kinetics of heavy metals from tannery effluent using composite agricultural waste. *Arid Zone Journal of Engineering, Technology & Environment*, 21(1), 270-278.
[17]. Raji, Z., Karim, A., Karam, A., & Khalloufi, S. (2023). Adsorption of heavy metals: mechanisms, kinetics, and applications of various adsorbents in wastewater remediation—A review. *Waste*, 1, 775–805.
[18]. Tahir, T., Druteikienė, R., Žukauskaitė, Z., Vaičiūnienė, J., Selskiene, A., Ignatjev, I., & Adnan, M. (2026). Biosorption of Lead (II) and cadmium (II) ions from aqueous solution by buckwheat (Fagopyrum Esculentum) hulls biosorbent: kinetic, equilibrium and thermodynamic studies. *Chemical Physics*, 602, 112997.
[19]. Ukpaka, C. & Agunwamba, J.C. (2023). Comparative analysis of tracer studies in the determination of longitudinal dispersion coefficients. Water Science and Technology. 89(9): 2209-2224.
[20]. Yousif, S.A., & Al-Mosawi, S. (2022). Adsorptive separation of dissolved cadmium from aqueous solution using (*Ziziphus Spina-Christi*) leaves as an adsorbent. *South African Journal of Chemical Engineering*, 42, 12-22.
[21]. Zand, A.D., & Abyaneh, M.R. (2020). Adsorption of Lead, manganese, and copper onto biochar in landfill leachate: implication of non-linear regression analysis. *Sustainable Environment Research*, 30, 18.

@IJAERD-2026, All rights Reserved